

## MICROWAVE PROPERTIES OF FERROELECTRIC THIN FILMS

J. M. POND, S. W. KIRCHOEFER, W. CHANG, J. S. HORWITZ,  
and D. B. CHRISEY  
Naval Research Laboratory, Washington, DC 20375-5347, USA

The microwave properties of ferroelectric thin films are being investigated. Interdigitated capacitors fabricated on ferroelectric thin films of  $\text{Sr}_{0.5}\text{Ba}_{0.5}\text{TiO}_3$  have been characterized at room temperature from 50 MHz to 20 GHz. The relative dielectric constant and dielectric loss tangent of the ferroelectric thin film are then extracted using a conformal-mapping based approach. For large dielectric constants the upper frequency limit for which the conformal-mapping technique is valid can be as low as 5 GHz. This information is being used to optimize the ferroelectric film deposition process for microwave device application. Results indicate that this technology will compare favorably with conventional varactors above a few GHz, and should be useful for tunable microwave circuits in some 300 K applications.

**Key words:** ferroelectric; varactor; interdigitated capacitor

### INTRODUCTION

It has long been known that the electric field dependence of the dielectric constant of ferroelectric materials could be useful in making tunable microwave devices and circuits<sup>[1-3]</sup>. Recently, there has been considerable effort in developing the pulsed-laser deposition technique to grow ferroelectric thin films that have the necessary material and electronic properties for tunable microwave electronic components<sup>[4]</sup>. Through considerable efforts in optimizing deposition, annealing, and doping

conditions it has been possible to realize ferroelectric thin films which retain a large dependence of the susceptibility on the applied electric field with acceptably low losses for some microwave applications. This paper reports results for interdigitated thin-film capacitors that have been fabricated on thin films of  $\text{Sr}_{0.5}\text{Ba}_{0.5}\text{TiO}_3$ . This composition results in a Curie temperature slightly below room temperature, and films that exhibit large dielectric constant dependence on electric field.

### DEVICE FABRICATION

The pulsed-laser deposition technique used for the formation of these ferroelectric films has been described extensively in prior work<sup>[5-6]</sup>. An excimer laser is used to vaporize material from a high-density sintered target of compressed powder, containing the stoichiometric ratios necessary for the desired film. A (100)  $\text{LaAlO}_3$  or  $\text{MgO}$  substrate is thermally sunk to a heated stainless steel stage with silver paint. The substrate is placed in close proximity to the sintered target so that as the pulsed laser ablates material from the target, the plume of material created is deposited on the substrate. Material is deposited on the substrate at a rate of 2 Å per laser pulse, to a desired thickness of approximately 0.4 µm. The resulting film is single-phase and (100) oriented. The film compositions and thicknesses are verified using Rutherford backscattering measurements<sup>[7]</sup>.

An array of interdigitated capacitors is fabricated on these films by photolithography and metal-lift-off patterning using a multi-level resist process. The multi-level resist process is required since, in order to minimize metallic losses in the interdigitated electrode structure at microwave frequencies, a thickness at least 1.5-µm of silver is employed. The desired pattern is first developed as windows in a tri-layer resist. The resist is composed of successive depositions of PMMA, a thin metal film, and Microposit 1818 photoresist. A mask with the desired pattern is used to expose and develop the 1818 resist. The pattern is transferred to the metal film by wet etching. The 1818 resist is removed by flood exposure and developing. Next, the sample is flood exposed by deep-UV in order to transfer the pattern to the PMMA. After the PMMA is developed, the sample is ready for the final metallization. At this point, the substrate surface is exposed only where the desired metal electrode structure is needed. Silver is deposited in an e-beam evaporator over the entire substrate, to a thickness of at least 1.5 µm, followed by a thin gold layer which preserves the surface for

electrical contact. Liftoff in acetone is used to delineate the capacitor pattern. A variety of device geometries are fabricated. Finger length varies from 15 to 125  $\mu\text{m}$ , and finger gap varies from 5 to 12  $\mu\text{m}$ . The total number of fingers in any individual device varies from 8 to 12. The devices are designed such that, given the expected relative dielectric constant of the ferroelectric film, the resultant device capacitances will be on the order of a picofarad.

### MEASUREMENTS

The interdigitated capacitors are measured as a function of frequency and bias field to determine their capacitance, tuning, and device quality factor ( $Q$ ). The devices are connected via 200- $\mu\text{m}$  pitch Picoprobe microwave probe to an HP 8510C vector network analyzer, and microwave reflection measurements ( $S_{11}$ ) are performed. Dc bias is applied to the capacitor under test through the internal bias tees of the network analyzer test set. The device bias is set initially at -40 volts, and swept in 5-volt steps to +40 volts, and then back to -40 volts. The 40-volt limit is imposed on the experiment by the limitations of the bias tees of the network analyzer, and does not represent any inherent breakdown limitation of the devices. Data are collected at 401 frequency points in the range from 50 MHz to 20 GHz. The dc-bias network is capable of measuring low-frequency resistance and reactance, as well as supplying the needed bias voltages. Data on both the dc characteristics and microwave  $S_{11}$  measurements are collected for each bias point, and stored in computer files for data reduction and analysis. Since the metallization losses are small enough to be ignored, the data are fitted to a parallel resistor-capacitor model to determine the device capacitance and  $Q$ . In order to demonstrate the applicability of this broadband measurement approach, it is useful to consider the simulated response of a 1 pF capacitor for different loss tangents. Figure 1 shows the computed reflection coefficients for such a capacitor for different values of a frequency independent loss tangent. As can be seen, the device  $Q$  is easily resolvable for values of  $Q$  less than about 100. In fact, the resolution of the measurement is higher than can be demonstrated in Figure 1 and this broadband technique is useful for  $Q$  values up to 500.

Since the primary loss mechanism is expected to be due to the dielectric loss tangent of the ferroelectric, the device is modeled as a bias dependent ideal capacitor in parallel with a bias dependent and frequency dependent resistance. With devices such as this one that exhibit relatively low loss, the difference between values of capacitance and  $Q$  for a series resistor-capacitor

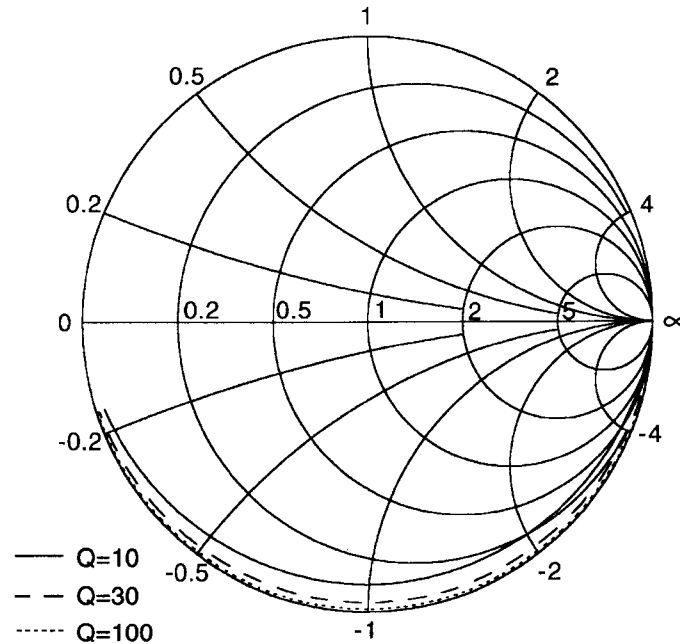


FIGURE 1 Plot of the reflection coefficient ( $S_{11}$ ) on the Smith Chart for a 1 picofarad capacitor over the frequency range from 100 MHz to 10 GHz for different values of device quality factor.

model versus a parallel resistor-capacitor model is not significant. For devices that have significant losses, a parallel network shows the best fit to that experimental data, and so a parallel model is used. If the metal film losses of the capacitor were dominant, a series resistance element would be necessary. However, measurements of calibration devices fabricated on standard low loss dielectric substrates have shown that the metal film resistance losses are negligible relative to the dielectric losses observed in the ferroelectric thin films, and so a series loss element is not needed in the model. Since the reflection measurements are all performed at low microwave power levels the extracted device parameters are small-signal in nature. Although dc hysteresis is evident in some devices, for many microwave circuit applications requiring

a tunable reactance, the small-signal lumped-element model applied herein is sufficient as long as the losses are considered to be bias dependent.

Whereas microwave circuit design issues can be adequately addressed by parameterizing device capacitance and Q versus bias, quantifying the relative dielectric constant and loss tangent of the ferroelectric thin film is important in understanding and optimizing these materials for device applications. A pseudo-static model has been used successfully to determine the dielectric constant of the ferroelectric thin film from the measured interdigitated capacitor data <sup>[8]</sup>.

## RESULTS

For the device to be examined in detail, three  $S_{11}$  reflection data curves are shown in Figure 2. These curves are for 0, 20, and 40 Volts dc bias, over the frequency range from 200 MHz to 20 GHz. The dimensions of this capacitor are; finger overlap length of 115  $\mu\text{m}$ , finger width of 10  $\mu\text{m}$ , and gap of 7.5  $\mu\text{m}$ . The ferroelectric thin film is  $\text{Sr}_{0.5}\text{Ba}_{0.5}\text{TiO}_3$  with a thickness of 0.4  $\mu\text{m}$  on a 508  $\mu\text{m}$ -thick single crystal MgO substrate. The departure from expected capacitor-like response observed near the short-circuit point on the Smith chart occurs at the upper end of the frequency sweep. This significant departure from discrete device behavior is a result of the wavelength in the dielectric approaching the dimensions of the device geometry due to the high relative dielectric constant of the ferroelectric thin film. As a result the device is no longer electrically small and the lumped-element model employed is no longer applicable. To avoid introducing this error into the lumped-element models, data that exhibit such departure from discrete device behavior are not used to extract the dielectric properties of the ferroelectric thin-film. The useful upper measurement range can be as low as 5 GHz for devices fabricated with our standard mask set.

Using the  $S_{11}$  data shown in Figure 2, and the lumped element model that has been assumed results in capacitance versus frequency curves for different bias points as shown in Figure 3. Obviously the lumped element model is not valid above about 5 GHz for this device. Above 5 GHz the device must be described as a distributed circuit. Although a detailed circuit model incorporating these effects is beyond the scope of this paper, it should be noted that the distributed circuit model would be that of a transmission line which is capacitively coupled at each end. Since the phase velocity of a trans-

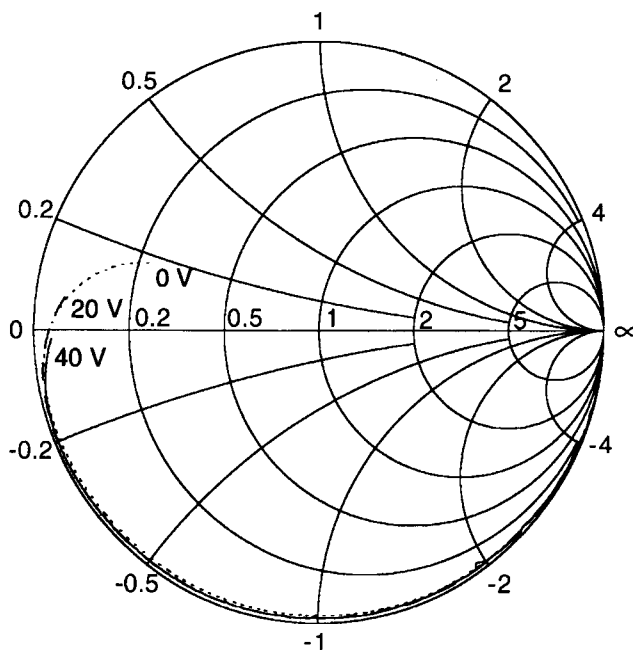


FIGURE 2 Plot of the reflection coefficient ( $S_{11}$ ) on the Smith Chart for a ferroelectric interdigitated capacitor at 0, 20, and 40 volts bias over the frequency range from 0.2 to 20 GHz. The data spans from the open-circuit point (at the right) at low frequencies to near the short-circuit point (at the left) at high frequencies.

mission line is inversely proportional to the square root of the capacitance per unit length, the frequency dependent behavior of the response, indicated by the shift in the capacitance peak in Figure 3, as a function of applied bias, should be related to the low frequency tuning range of the capacitance. By focusing attention on the shift in the peak of the capacitance curves with bias it can be seen that this relationship is correct; the square root of the ratio of the low frequency capacitances is precisely the ratio in the frequency shift of the capacitance peaks at high frequencies.

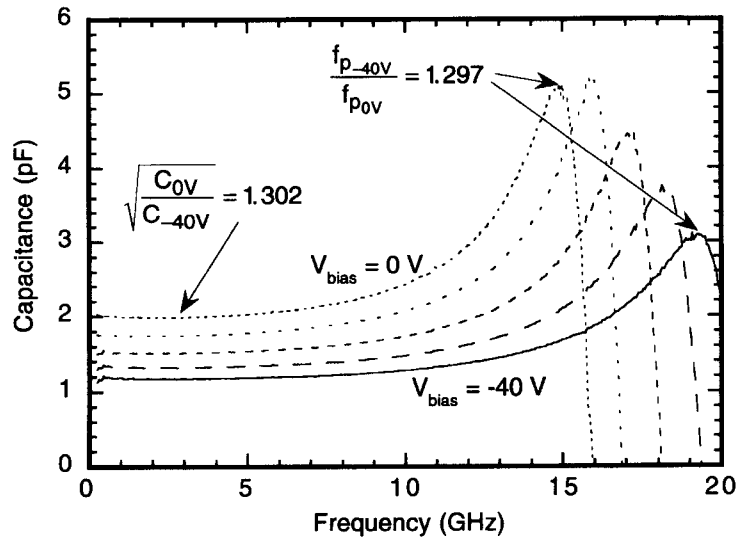


FIGURE 3 Capacitance versus frequency at various bias voltages (10 Volt steps) for a ferroelectric interdigitated capacitor.

Analyzing the data of Figure 2 using the lumped element circuit model results in the capacitance versus bias for different frequencies and  $Q$  versus frequency for different biases shown in Figures 4 and 5, respectively. The capacitance curves displayed in Figure 4 are calculated at 2 GHz intervals from data taken over the frequency range from 1 to 5 GHz. Figure 5 displays the curves for  $Q$  calculated from the same data set but are shown as a function of frequency for several biases. As expected, there is some residual hysteresis with bias voltage which can be seen if the bias is swept continuously back through the voltage range in the opposite direction. Note the slight hysteresis evident in the data even though the Curie temperature of the film is known to be well below room temperature. Figure 5 shows that the device  $Q$  is frequency dependent as well as bias dependent even in the regime where electrical size effects can be neglected. This behavior is a direct consequence of the bias and frequency dependence of the dielectric loss tangent of the ferroelectric thin film since the metal losses of the interdigitated electrode are known to be much smaller and hence, if dominant, the  $Q$  would be much higher.

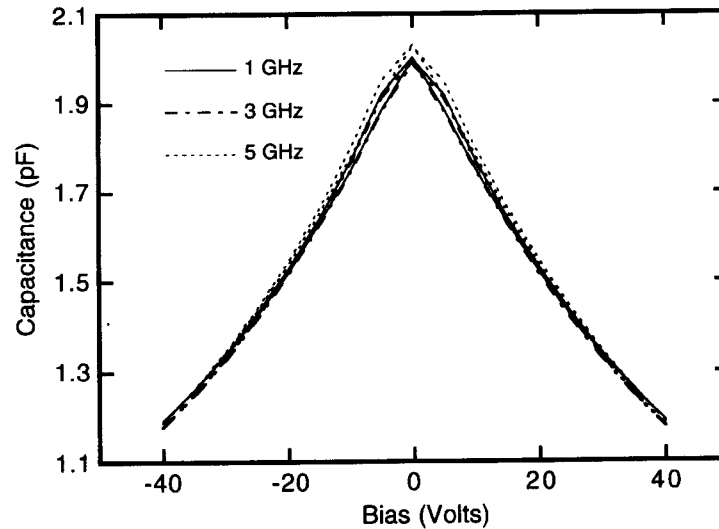


FIGURE 4 Capacitance versus bias voltage of a ferroelectric capacitor with for frequency values of 1, 3, and 5 GHz. The data represents bias swept for -40 to 40 to -40 volts.

Conformal-mapping based models for interdigitated capacitors on layered substrates<sup>[8]</sup> have been applied to our device data. By definition, these models are only applicable at frequencies which are sufficiently low that the device is electrically small. Using this approach, the relative dielectric constant of the ferroelectric thin film can be calculated given the geometry of the interdigitated capacitor, the thickness of the ferroelectric thin film, the thickness and dielectric constant of the substrate and the measured capacitance. Figure 6 shows, for the measured data shown in Figure 2, the relative dielectric constant of the ferroelectric thin film varying from 1750 at 0 V bias to 1000 at 40 V bias. Although the conformal mapping based model is only valid when the device is electrically small, it is found that the values extracted from the capacitances vary by only  $\pm 5\%$  up to 5 GHz. From Figure 3 it can be seen that the capacitance tuning ratio is  $\sim 1.7:1$  from 0 to 40 Volts while the dielectric constant ratio is slightly larger over the same bias range. This follows from the fixed capacitances, the substrate below and the air above, which, in parallel with the ferroelectric thin film, constitute the total

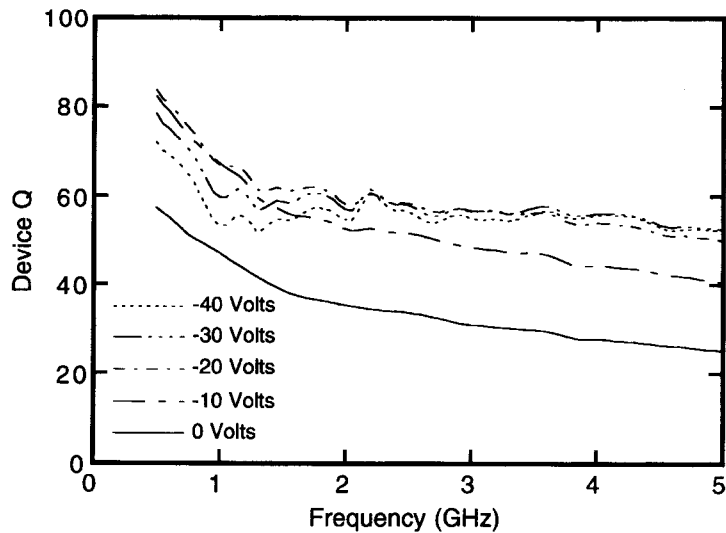


FIGURE 5 Ferroelectric interdigitated capacitor device  $Q$  versus frequency for various bias voltages. The change in slope of device  $Q$  with frequency between 1 and 2 GHz has been observed in several devices.

device capacitance. Since the difference in tuning range is very small it can be assumed that only a small percentage of the electric energy is stored outside the ferroelectric film. Using the calculated 0 V ferroelectric relative dielectric constant and assuming the guided wave effective dielectric constant is given by the ferroelectric dielectric, we note that the wavelength at 10 GHz is approximately 0.7 mm. Since the finger overlap length (115  $\mu\text{m}$ ) is considerably greater than a tenth of a wavelength it is to be expected that the lumped element model is invalid at the upper end of our measurements. Figure 7 shows the dielectric loss tangent of the ferroelectric film versus frequency for several bias voltages. The loss tangent values are slightly higher than the reciprocal of the device  $Q$  since the parallel parasitic capacitances of the air and MgO substrate are lossless in comparison. Efforts are underway to understand the bias and frequency dependencies of the ferroelectric loss tangent on the ferroelectric film deposition conditions and microscopic properties. It should be noted in Figure 7 that there appears to be a change in

the slope of the loss tangent versus frequency at approximately 1.5 GHz. Although this behavior is not anomalous to this particular device, neither is it seen universally in our films. This behavior occurs more frequently in low loss films that retain some tunability. Although slight errors in system calibration could produce such results, measurements of devices fabricated on bulk low loss substrates do not exhibit this behavior. Thus, it must be concluded that this behavior is an intrinsic property of the interdigitated capacitor, although it may not be an intrinsic property of the ferroelectric film.

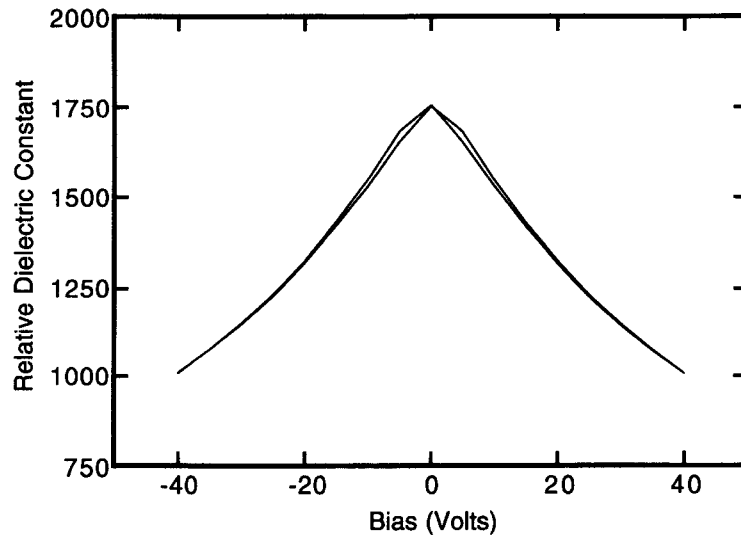


FIGURE 6 Relative dielectric constant at 3 GHz of the ferroelectric thin film versus bias as computed from the reflection coefficient data using the conformal-mapping based approach. Since the conformal-mapping approach is a pseudo-static approximation and the data in Figure 3 shows the device capacitance to be flat up to 5 GHz, the relative dielectric constant at any other frequency up to 5 GHz would be indistinguishable from the 3 GHz values.

The electrical size effects evident above 5 GHz are not a cause for concern for most microwave applications. There is little utility for operating

varactors with impedance values that are so close to an apparent short circuit. Many applications require capacitors which are designed to operate in the regime where these capacitors can be regarded as electrically-small devices. Either scaling down the designed capacitance or operating at a lower frequency will minimize the size-related effects and result in useful devices. Thus, the anomalous behavior seen at high frequencies does not present a serious limitation for practical application of this technology.

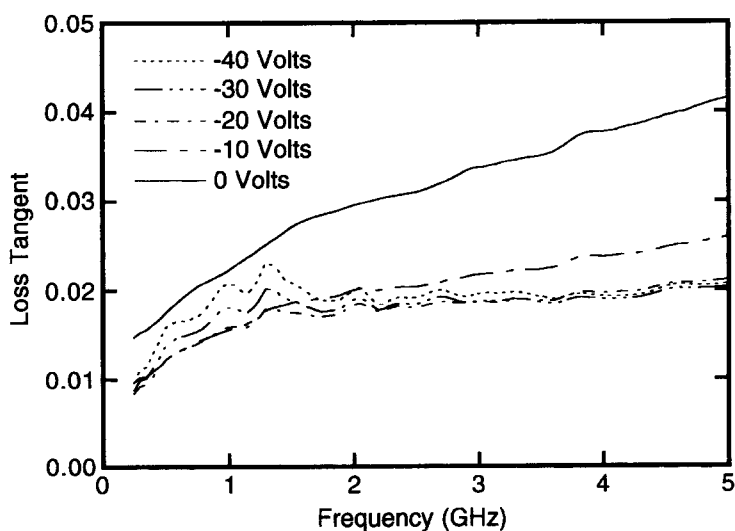


FIGURE 7 Loss tangent of the ferroelectric film versus frequency for several bias voltages. The loss tangent values are slightly higher than the reciprocal of the device  $Q$  since the parallel parasitic capacitances of the air and MgO substrate are lossless in comparison.

## CONCLUSIONS

We have fabricated varactors, from ferroelectric thin films of  $\text{Sr}_{0.5}\text{Ba}_{0.5}\text{TiO}_3$  on MgO substrates, which have reasonable tuning ranges and which have losses that are sufficiently low for some microwave circuit applications at room temperature. These devices demonstrate considerably-improved

characteristics over previous devices made in the same facility. For frequencies in excess of 10 GHz, these results are comparable to what is achieved by other conventional varactor technologies. Deviations from ideal discrete capacitor behavior have been shown to be a direct result of the extremely high dielectric constants associated with these materials.

#### **Acknowledgment**

The authors wish to acknowledge the technical assistance of W. W. Moore and the helpful discussions of L. A. Knauss and C. Rauscher. This work was funded by the Office of Naval Research and SPAWAR.

#### **References**

- [1.] V. K. Varadan, D. K. Gohdgaonkar, V. V. Varadan, J. F. Kelly, and P. Glikerdas, *Microwave Journal*, **35**, no. 1, 116-127 (1992).
- [2.] V. Chivukula, J. Ilowski, I. Emesh, D. McDonald, P. Leung, and M. Sayer, *Integr. Ferroelectr.*, **10**, no. 1-4, 247 (1996).
- [3.] A. Outzourhit, J. U. Trefny, T. Kito, B. Yarar, A. Naziripour, and A. M. Hermann, *Thin Solid Films*, **259**, no. 2, 218 (1995).
- [4.] J. S. Horwitz, D. B. Chrisey, J. M. Pond, R. C. Y. Auyeung, C. M. Cotell, K. S. Grabowski, P. C. Dorsey, and M. S. Kluskens, *Integr. Ferroelectr.*, **8**, no. 1-2, 53 (1995).
- [5.] K. S. Grabowski, J. S. Horwitz, and D. B. Chrisey, *Ferroelectrics*, **116**, no.1-2, 19 (1991).
- [6.] J. S. Horwitz, D. B. Chrisey, K. S. Grabowski, and P. E. Leuchtner, *Surf. Coat. and Technol.*, **51**, no.1-3, 290 (1992).
- [7.] L. A. Knauss, J. S. Horwitz, D. B. Chrisey, J. M. Pond, K. S. Grabowski, S. B. Qadri, E. P. Donovan, and C. H. Mueller, *Mater. Res. Soc. Symp. Proc.* **388**, 73 (1995).
- [8.] S. S. Gevorgian, T. Martinsson, P. I. J. Linner, and E. L. Kollberg, *IEEE Trans. Microwave Theory Tech.*, **44**, no. 6, 896, (1996).